The IRM Quarterly

ISSN: 2152-1972

Winter 2011, Vol. 20 No. 4

Inside...

Interpretation of Low-Temperature Data Part III: The Magnetite Verwey Transition (Part A)

Mike Jackson, Bruce Moskowitz, Julie Bowles, IRM

After completing his doctorate in chemistry at the University of Amsterdam in 1934, Evert Johannes Willem Verweij (aka Verwey) moved to the Philips Research Laboratories in Eindhoven, where he continued the research into the properties and behavior of colloids for which he is widely remembered today. In geophysics, of course, we remember Verwey primarily for his work in pursuit of another interest, the metal oxide spinels, their cation arrangements and associated physical properties. Specifically, magnetite (Fe_3O_4) undergoes a low-temperature transformation which is now known as the Verwey transition, in recognition of his important work on electrical conductivity variations with temperature and their implications for crystallography and cation distribution.

We now know (more or less) that at the Verwey transition temperature (T_V ~120 K), magnetite transforms from cubic ($T > T_V$) to monoclinic ($T < T_V$) symmetry. This transformation is related to changes in crystal symmetry and in cation ordering and is accompanied by dramatic changes in electrical conductivity and heat capacity. At a slightly higher temperature (~130 K), the first magnetocrystalline anisotropy constant (K_1) changes sign, and at this isotropic point (T_i) the easy directions of magnetization change from the [111] cubic body diagonals ($T > T_i$) to the [001] cube edge directions ($T_V < T < T_i$). In the transformation to the monoclinic phase ($T < T_V$) one of the cube edge orientations becomes the new c-axis, the unique easy magnetic orientation. As you might expect, the transition is often easily identified by magnetic measurements.

The Verwey transition is widely used for identification of magnetite in natural samples [e.g., Mauritsch & Turner, 1975], for cleaning of natural remanence by low-temperature demagnetization [e.g., Ozima et al., 1964; Merrill, 1970; Dunlop, 2003], and for recognition of magnetotactic bacteria in sediments [e.g., Moskowitz et al., 1989, 1993]. In spite of these useful applications of the Verwey transition and nearly a century of research, fundamental aspects of the transition and of the low-T state of magnetite are still incompletely understood, and competing theories remain embroiled in controversy [e.g., Walz, 2002; Garcia & Subias, 2004; Piekarz et al., 2007; Rozenberg et al., 2007].

Figure 1. Magnetite octohedra from Cerro Huanaquino, Bolivia. Photo by Rob Lavinsky, iRocks.com (via Wikipedia Commons).

In this article, the first in a series devoted to the Verwey transition, we will discuss some of the initial observations and history behind the transition, the fundamental ideas about magnetite's structure above and below T_V, and how this structure affects macroscopic physical properties. In subsequent articles we will explore the dependence of this transition and of the low-T phase on variables of interest including composition (cation deficiency and/or

cont'd. on pg. 7...

Summer School in Rock Magnetism

June 2011, Minneapolis, MN

Magnetic geoscience research uses sensitive, nondestructive measurements on natural materials to illuminate geomagnetic field history, tectonic processes and environmental changes. Learn more about the fundamentals and applications at the first biennial Summer School in Rock Magnetism (SSRM), which will be held from June 6-15, 2011 at the Institute for Rock Magnetism (IRM) in Minneapolis, MN.

Limited scholarships available thanks to the **AGU Geomagnetism and Paleomagnetism Section** and to the **National Science Foundation, Earth Science Division**.

More information on page 4...

Visiting Fellow's Reports

Magnetic fingerprint of La Plata plume inception into the Brazilian shelf

Grasiane L. Mathias
Department of Geophysics
University of São Paulo, Brazil
grasiane@iag.usp.br

The La Plata drainage basin is the main source of sediments to the western South Atlantic, delivering annually ~670 km³ of sediments into the ocean carried within their brackish waters. It comprises a catchment area of ~3,200,000 km² which encompasses a large surface of the Parana flood basalts. The cold, salt-poor waters of the La Plata plume may have reached latitudes as far north as 24° S [1]. But the influence of the La Plata plume on the sediment input in the region is probably younger than 6,000 years B.P., when the La Plata River was flooded as a result of the transgression succeeding the last glacial maximum [2]. Here the progressive inception of the La Plata water plume into the southeastern Brazil shelf is revealed by changes in magnetic properties along a two meters long sediment core collected at 25°30' S and 46°38' W.

The IO7610 piston core was collected at a water depth of about 100 m. It comprises laminated muddy sediments with fine sand, accumulated within the past 6,000 years with an average sedimentation rate of 35.6 cm yr^{-1}, deduced from six AMS radiocarbon ages along the core. Surface sediments (first 10 cm) were lost during coring. Samples for grain-size analyses were collected at 2 cm intervals, then frozen and subsequently freeze-dried. The sub-sampling for magnetic mineralogy analysis was performed using 8 cm^3 plastic boxes at regular intervals of 2 cm totaling 71 samples. Sampling conditions did not allow a continuous recovery of the sedimentary record for magnetic studies, leaving a gap between 86 and 114 cm.

Magnetic measurents were performed in the new 2G Enterprises pass-through SQUID magnetometer of the Institute for Rock Magnetism. Two artificial magnetizations were induced in the samples – the anhysteretic remanent magnetization (ARM) and the isothermal remanent magnetization (IRM). The ARM was acquired with a steady bias field of 0.05 mT up to 100 mT (ARM100) and subsequently demagnetized step by step in alternating fields (AF) up to 100 mT. The IRM was acquired at room temperature in a direct field of 1000 mT (IRM1000mT) and finally at a backfield of -300 mT (IRM-300). Bulk magnetic susceptibility (χ) was measured in all samples in the Kappabridge KLY-4/CS-4 (Agico Ltd.) of the Paleomagnetic Lab of the São Paulo University. The following magnetic parameters were calculated from ARM and IRM acquisitions: hard IRM (HIRM = [IRM_{1000} – IRM_{-300}]/2), ARM (%) (ARM_{10}/ARM_{100}) and S-Ratio ($-IRM_{-300}/IRM_{1000}$). Low-T thermomagnetic susceptibility curves, hysteresis measurements at room temperature, First Order Reverse Curves (FORC) and zero field cooled (ZFC) curves were performed in selected samples to better constrain the magnetic mineralogy.

Concentration-dependent magnetic parameters ARM, χ, IRM and HIRM (Fig. 1a, 1b, 1c and 1d) show a significant increase at the top of the core, suggesting an enhanced detrital input after 1,300 years B.P. Other magnetic parameters reveal more subtle changes in magnetic carriers throughout the core. Magnetite is present all along the core, being identified by typical Verwey transitions in ZFC curves, which also show a log-normal decay of magnetization in their first-derivative [7] that is typical of

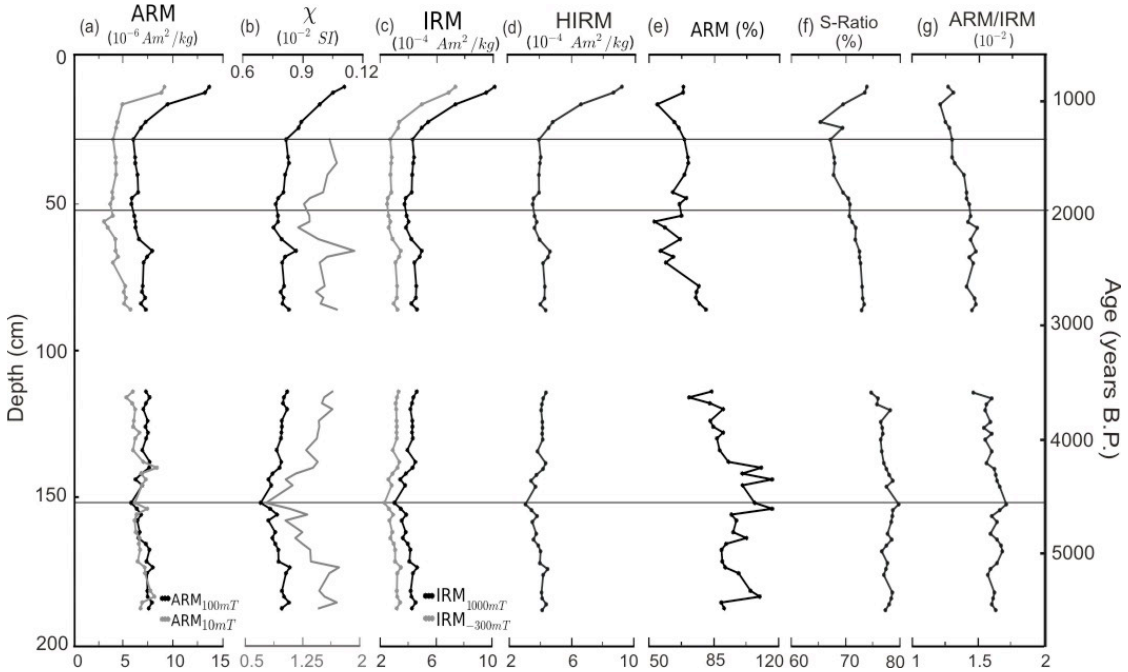

Figure 1. Magnetic parameters changes with depth (left axis) and age (right axis). a. ARM100mT and ARM10mT; b. χ (greece curve without top part evidences changes); c. IRM1000mT and IRM-300mT; d. HIRM; e. ARM%; f. S-Ratio (%); g. ARM/IRM.

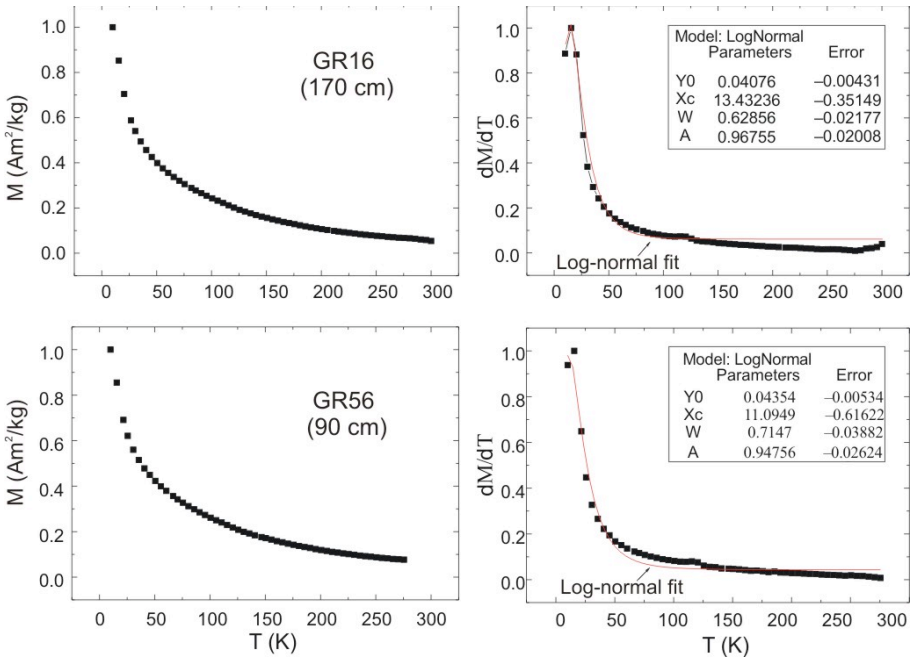

Figure 2: Zero-Field Cooled magnetization curves (a, b) and variation of magnetization using log-normal fit [7] (c, d) for samples GR16 and GR56.

superparamagnetic behavior (Fig. 2). Magnetite coercivity (and consequently grain-size) changes significantly along the core. This is clearly shown by the continuous decrease in the ARM (%) parameter between 152 cm and 54 cm depth, indicating a progressively higher contribution of low-coercivity magnetite grains (Fig. 1e). Hematite has also been identified in the core and accounts for the slight increase in remanence at high-fields in IRM acquisition curves. The S-Ratio is usually interpreted in terms of magnetite to hematite proportion. In the IO7610 core, it follows the same trend of ARM (%) and ARM/IRM parameters, indicating that hematite grains were preferentially deposited together with coarse magnetite grains (Fig. 1e, 1f and 1g).

The fluctuations in magnetic parameters can be used to track changes in clastic input. The transgression following the last glacial maximum flooded the Rio de La Plata river, hindering continental sediments from reaching the shelf (e.g. [1] , [3]). By that time, the sediments deposited on the Brazilian shelf were likely derived from the Argentinean shelf, being transported northward by a much stronger Malvinas current [4]. This current is presently blocked by the Rio de la Plata outflow. In our magnetic record, these Argentinean-derived sediments correspond to the basal interval, rich in fine-grained magnetite grains and devoid of more oxidized types. The continuous changes in magnetic properties upcore probably track the progressive inception of the La Plata plume, delivering coarser magnetic grains derived mostly from the weathering of magnetite-rich Parana flood basalts. These sediments are also enriched in other oxidized types, like hematite, thus explaining the coherence between ARM (%), ARM/IRM and S-Ratio parameters. The shift in these parameters occurs at ~4,700 years B.P. and set the time at which the influence of the La Plata plume reached the 25°S latitude of the IO7610 core. The final shift in magnetic properties is marked by a strong increment in concentration-dependent parameters between 1,300 and 915 years BP, and coincides with an increase in humidity at the La Plata drainage basin [5]. This increase in precipitation was responsible for the onset of the de La Plata delta [6] delivering a higher amount of detrital magnetic material to the ocean. In summary, environmental magnetic indicators are fully compatible with the paleoceanographic and paleoclimatic record in the SE margin of South America. They suggest that sedimentation on the Brazilian continental shelf at the latitude of IO7610 core in the past 6,000 years B.P. was mainly controlled by changes in sea-level and continental climate, which affected the relative input of sediments from two sources – the Argentinean continental shelf and the La Plata plume.

I would like to thank the IRM for providing full access to the laboratory, all staff of the IRM for their help and warmth, and especially Mike Jackson and Julie Bowles for their valuable discussions.

References

[1] Mahiques, M. M., Wainer, I. K., Burone, L., Nagai, R., Mello e Sousa, S. H., Figueira, R. C., et al. (2009), *Quat. Int.*, 206, 52-61. **[2]** Violante, R. A., & Parker, G. (2004), *Quat. Int.*, 114, 167-181. **[3]** Zárate, M., Kemp, R., & Toms, P. (2009), *J. S. Am. Earth Sci.*, 27, 88-99. **[4]** Mahiques, M. M., Tassinari, C. C., Marcolini, S., Violante, A., R., Figueira, R. C., et al. (2008), *Mar. Geol.*, 250, 51-63. **[5]** Tonni, E. P., Cione, A. L., & Figini, A. J. (1999), *Palaeogeogr. Palaeoclimatol. Palaeoecol.*, 147, 257-281. **[6]** Cavalotto, J. L., Violante, R. A., & Parker, G. (2004), *Quat. Int.*, 114, 155-165. **[7]** Vasquez, C.A., Orgeira, M.J., & Sinito, A.M. (2009), *Environ. Geol.*, 56, 1653-1661.

Application deadline for 2011 Visiting Fellows (Jul - Dec): April 30

Visit www.irm.umn.edu/IRM/Visiting.html for new application forms and instructions.

2011 Summer School for Rock Magnetism

A Community Based Program for Training the Next Generation of Paleomagnetists

Magnetic geoscience research uses sensitive, nondestructive measurements on natural materials to illuminate geomagnetic field history, tectonic processes and environmental changes. Learn more about the fundamentals and applications at the first biennial Summer School in Rock Magnetism (SSRM), which will be held from June 6-15, 2011 at the Institute for Rock Magnetism (IRM) in Minneapolis, MN. The 10-day program is targeted at graduate students and advanced undergraduate students in rock magnetism, paleomagnetism, and associated fields. Students will receive intensive instruction in rock magnetic theory and laboratory techniques. A daily schedule of lectures, hands-on laboratory measurements, and data processing will introduce students to the fundamentals of rock magnetism and paleomagnetism and the practical aspects of collecting and interpreting data responsibly. Instructors for the summer school will be primarily IRM Faculty and staff.

Participant costs will include a $100 registration fee, housing ($231 for 11 nights), meals, and travel to and from Minneapolis. Housing will be available in the dormitories on the University of Minnesota campus. Limited kitchen facilities are available in the dorms, or meals may be purchased in the dormitory dining hall or in many reasonably-priced dining establishments on or near campus. A limited number of scholarships ($200-$250, maximum $500) will be awarded to help cover some of the costs of participating. Scholarships are thanks to the support of the **National Science Foundation, Earth Science Division** and the **American Geophysical Union, Geomagnetism & Paleomagnetism Section**.

Registration will be limited to a maximum of 20 students, in the order in which payment is received. Refunds will be subject to a $50 cancellation fee. Applications must be received by the deadline, March 25, 2011. Note that as of press time, we are now accepting waiting list applications.

For registration and payment information, visit the IRM website at http://www.irm.umn.edu/. For questions or more information, send e-mail to irm@umn.edu.

The *IRM Quarterly* is always available as a full color pdf online at www.irm.umn.edu

Current Articles

A list of current research articles dealing with various topics in the physics and chemistry of magnetism is a regular feature of the IRM Quarterly. Articles published in familiar geology and geophysics journals are included; special emphasis is given to current articles from physics, chemistry, and materials-science journals. Most abstracts are taken from INSPEC (© Institution of Electrical Engineers), Geophysical Abstracts in Press (© American Geophysical Union), and The Earth and Planetary Express (© Elsevier Science Publishers, B.V.), after which they are subjected to Procrustean culling for this newsletter. An extensive reference list of articles (primarily about rock magnetism, the physics and chemistry of magnetism, and some paleomagnetism) is continually updated at the IRM. This list, with more than 10,000 references, is available free of charge. Your contributions both to the list and to the Abstracts section of the IRM Quarterly are always welcome.

Magnetic Fabrics and Anisotropy

Mamtani, M. A., and P. Sengupta (2010), Significance of AMS analysis in evaluating superposed folds in quartzites, *Geol. Mag.*, 147, 910-918.

Roperch, P., V. Carlotto, and A. Chauvin (2010), Using anisotropy of magnetic susceptibility to better constrain the tilt correction in paleomagnetism: A case study from southern Peru, *Tectonics*, 29, TC6005, doi:10.1029/2009TC002639.

Till, J., M. Jackson, and B. Moskowitz (2010), Remanence stability and magnetic fabric development in synthetic shear zones deformed at 500 degrees C, *Geochem. Geophys. Geosys.*, 11, Q12Z21, doi:10.1029/2010GC003320.

Vishnu, C., M. Mamtani, and A. Basu (2010), AMS, ultrasonic P-wave velocity and rock strength analysis in quartzites devoid of mesoscopic foliations - implications for rock mechanics studies, *Tectonophysics*, 494(3-4), 191-200.

Archeomagnetism

Ben-Yosef, E., L. Tauxe, and T. Levy (2010), Archaeomagnetic dating of copper smelting site f2 in the Timna Valley (Israel) and its implications for the modelling of ancient technological developments, *Archaeometry*, 52, 1110-1121.

Charvátová, I., J. Klokočník, J. Kolmaš and J. Kostelecky (2010), Chinese tombs oriented by a compass: Evidence from paleomagnetic changes versus the age of tombs, *Stud. Geophys. Geod.*, 55, 159-174.

Lengyel, S. (2010), The pre-AD 585 extension of the US Southwest archaeomagnetic reference curve, *J. Archaeolog. Sci.*, 37, 3081-3090.

Pineda Duran, M., A. Goguitchaichvili, J. Morales, B. Aguilar Reyes, L.M. Alva Valdiva, A. Oliveros-Morales, M. Calvo-Rathert, T. Gonzalez Moran, J. Robles-Camacho (2010), Magnetic properties and archeointensity of Earth's magnetic field recovered from El Opeño, earliest funeral architecture known in western Mesoamerica, *Stud. Geophys. Geod.*, 54, 575-593.

Spatharas, V., D. Kondopoulou, E. Aidona and K.G. Efthimiadis (2011), New magnetic mineralogy and archaeointensity results from Greek kilns and baked clays, *Stud. Geophys. Geod*, 55, 131-157.

Stark, F., J. Cassidy, M. J. Hill, J. Shaw, and P. Sheppard (2010), Establishing a first archaeointensity record for the SW Pacific, *Earth Planet. Sci. Lett.*, 298, 113-124.

Velraj, G., A. Musthafa, K. Janaki, K. Deenadayalan, and N. Basavaiah (2010), Estimation of firing temperature and ancient geomagnetic field intensity of archaeological potteries recently excavated from Tamilnadu, India, *Appl. Clay Sci.*, 50, 148-153.

Bio(geo)magnetism

Carlut, J., K. Benzerara, H. Horen, N. Menguy, D. Janots, N. Findling, A. Addad, and I. Machouk (2010), Microscopy study of biologically mediated alteration of natural mid-oceanic ridge basalts and magnetic implications, *J. Geophys. Res*., 115, G00G11, doi:10.1029/2009JG001139.

Lund, S., E. Platzman, N. Thouveny, G. Camoin, F. Corsetti, and W. Berelson (2010), Biological control of paleomagnetic remanence acquisition in carbonate framework rocks of the Tahiti coral reef, *Earth Planet. Sci. Lett*., 298, 14-22.

Environmental Magnetism / Paleoclimate Proxies

Boyle, J., J. Dearing, A. Blundell, and J. Hannam (2010), Testing competing hypotheses for soil magnetic susceptibility using a new chemical kinetic model, *Geology*, 38, 1059-1062.

Chaparro, M., D. Marie, C. Gogorza, A. Navas, and A. M. Sinito (2010), Magnetic studies and scanning electron microscopy - X-ray energy dispersive spectroscopy analyses of road sediments, soils and vehicle-derived emissions, *Stud. Geophys. Geod*., 54, 633-650.

Da Silva, A., V. Costanzo-Alvarez, N. Hurtado, M. Aldana, G. Bayona, O. Guzman, and D. Lopez-Rodriguez (2010), Possible correlation between Miocene global climatic changes and magnetic proxies, using neuro fuzzy logic analysis in a stratigraphic well at the Llanos foreland basin, Colombia, *Stud. Geophys. Geod*., 54, 607-631.

Edgar, K. M., P. Wilson, P. Sexton, S. Gibbs, A. Roberts, and R. Norris (2010), New biostratigraphic, magnetostratigraphic and isotopic insights into the Middle Eocene Climatic Optimum in low latitudes, *Palaeogeogr. Palaeoclimatol. Palaeoecol*., 297, 670-682.

Font, E., C. Nascimento, R. Omira, M. Baptista, and P. Silva (2010), Identification of tsunami-induced deposits using numerical modeling and rock magnetism techniques: A study case of the 1755 Lisbon tsunami in Algarve, Portugal, *Phys. Earth Planet. Int.*, 182, 187-198.

Hatfield, R., M. Cioppa, and A. Trenhaile (2010), Sediment sorting and beach erosion along a coastal foreland: Magnetic measurements in Point Pelee National Park, Ontario, Canada, *Sedimentary Geology*, 231, 63-73.

Liu, Q. S., J. Torrent, H. Morras, A. Hong, Z. Jiang, and Y. Su (2010), Superparamagnetism of two modern soils from the northeastern Pampean region, Argentina and its paleoclimatic indications, *Geophys. J. Int.*, 183, 695-705.

Ricordel-Prognon, C., F. Lagroix, M. G. Moreau, and M. Thiry (2010), Lateritic paleoweathering profiles in French Massif Central: Paleomagnetic datings, *J. Geophys. Res*., 115, B10104, doi:10.1029/2010JB007419.

Zhang, R., V. Kravchinsky, R. X. Zhu, and L. P. Yue (2010), Paleomonsoon route reconstruction along a W-E transect in the Chinese Loess Plateau using the anisotropy of magnetic susceptibility: Summer monsoon model, *Earth Planet. Sci. Lett.*, 299, 436-446.

Extraterrestrial Magnetism

Bezaeva, N., D. Badjukov, P. Rochette, J. Gattacceca, V. Trukhin, E. Kozlov, and M. Uehara (2010), Experimental shock metamorphism of the L4 ordinary chondrite Saratov induced by spherical shock waves up to 400 GPa, *Meteorit. Planet. Sci*., 45, 1007-1020.

Cassata, W., D. Shuster, P. Renne, and B. Weiss (2010), Evidence for shock heating and constraints on Martian surface temperatures revealed by Ar-40/Ar-39 thermochronometry of Martian meteorites, *Geochim. Cosmochim. Acta*, 74, 6900-6920.

Gattacceca, J., M. Boustie, L. Hood, J. P. Cuq-Lelandais, M. Fuller, N. Bezaeva, T. De Resseguier, and L. Berthe (2010), Can the lunar crust be magnetized by shock: Experimental groundtruth, *Earth Planet. Sci. Lett.*, 299, 42-53.

Tsunakawa, H., H. Shibuya, F. Takahashi, H. Shimizu, M. Matsushima, A. Matsuoka, S. Nakazawa, H. Otake, and Y. Iijima (2010), Lunar Magnetic Field Observation and Initial Global Mapping of Lunar Magnetic Anomalies by MAP-LMAG Onboard SELENE (Kaguya), *Space Sci. Rev*., 154, 219-251.

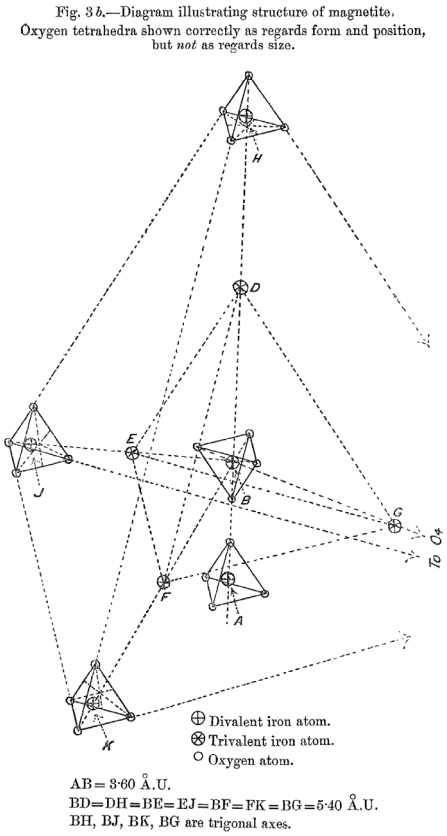

Fig. 3 *b*.—Diagram illustrating structure of magnetite. Oxygen tetrahedra shown correctly as regards form and position, but *not* as regards size.

From Bragg, W.H. (1915), The structure of the spinel group of crystals, Phil. Mag., 30, 305-315.

Geomagnetism and Geodynamo Studies

Aubert, J., J. Tarduno, and C. Johnson (2010), Observations and Models of the Long-Term Evolution of Earth's Magnetic Field, *Space Sci. Rev*., 155, 337-370.

Bogue, S. W., and J. Glen (2010), Very rapid geomagnetic field change recorded by the partial remagnetization of a lava flow, *Geophys. Res. Lett.*, 37, L21308, doi:10.1029/2010GL044286.

Donadini, F., M. Korte, and C. Constable (2010), Millennial Variations of the Geomagnetic Field: from Data Recovery to Field Reconstruction, *Space Sci. Rev*., 155, 219-246.

Finlay, C. et al. (2010), International Geomagnetic Reference Field: the eleventh generation, *Geophys. J. Int*., 183, 1216-1230.

Gromme, S., E. Mankinen, and M. Prevot (2010), Time-averaged paleomagnetic field at the equator: Complete data and results from the Galapagos Islands, Ecuador, *Geochem. Geophys. Geosys.*, 11, Q11009, doi:10.1029/2010GC003090.

Gubbins, D. (2010), Terrestrial Magnetism: Historical Perspectives and Future Prospects, *Space Sci. Rev*., 155, 9-27.

Pavon-Carrasco, F. J., M. Osete, and J. Torta (2010), Regional modeling of the geomagnetic field in Europe from 6000 to 1000 BC, *Geochem. Geophys. Geosys.*, 11, Q11008, doi:10.1029/2010GC003197.

Paleointensity Records and Methods

Barletta, F., G. St-Onge, J. Stoner, P. Lajeunesse, and J. Locat (2010), A high-resolution Holocene paleomagnetic secular variation and relative paleointensity stack from eastern Canada, *Earth Planet. Sci. Lett*., 298, 162-174.

Fabian, K., and R. Leonhardt (2010), Multiple-specimen absolute paleointensity determination: An optimal protocol including pTRM normalization, domain-state correction, and alteration test, *Earth Planet. Sci. Lett*., 297, 84-94.

Morales, J., X. Zhao, and A. Goguitchaichvili (2010), Geomagnetic field intensity from Kilauea 1955 and 1960 lava flows: Towards a better understanding of paleointensity, *Stud. Geophys. Geod*., 54, 561-574.

Shcherbakova, V., V. Shcherbakov, Y. Bretshtein, and G. Zhidkov (2010), Paleointensity and paleodirection of the geomagnetic field in the middle Miocene: Evidence from late Cenozoic volcanites of Primorye, *Izv. Phys. Solid Earth*, 46, 1035-1051.

Rock and Mineral Magnetism

Dietze, F., A. Kontny, I. Heyde and C. Vahle (2011), Magnetic anomalies and rock magnetism of basalts from Reykjanes (SW-Iceland), *Stud. Geophys. Geod*., 55, 109-130.

Dunlop, D. J., O. Ozdemir, and V. Costanzo-Alvarez (2010), Magnetic properties of rocks of the Kapuskasing uplift (Ontario, Canada) and origin of long-wavelength magnetic anomalies, *Geophys. J. Int.*, 183, 645-658.

Perez-Cruz, L., and J. Urrutia-Fucugauchi (2010), Characterization of distal turbidites in marine sedimentary sequences using magnetic mineral data and factor analysis of microfossils assemblages, *Stud. Geophys. Geod*., 54, 595-606.

Riquier, L., O. Averbuch, X. Devleeschouwer, and N. Tribovillard (2010), Diagenetic versus detrital origin of the magnetic susceptibility variations in some carbonate Frasnian-Famennian boundary sections from Northern Africa and Western Europe: implications for paleoenvironmental reconstructions, *Int. J. Earth Sci.*, 99, S57-S73.

Wang, X. S., R. Lovlie, X. Zhao, Z. Yang, F. Jiang, and S. Wang (2010), Quantifying ultrafine pedogenic magnetic particles in Chinese loess by monitoring viscous decay of superparamagnetism, *Geochem. Geophys. Geosys*., 11, Q10008.

Wang, R., and R. Lovlie (2010), Subaerial and subaqueous deposition of loess: Experimental assessment of detrital remanent magnetization in Chinese loess, *Earth Planet. Sci. Lett.*, 298, 394-404.

Zan, J. B., X. M. Fang, S. Yang, J. S. Nie, and X. Li (2010), A rock magnetic study of loess from the West Kunlun Mountains, *J. Geophys. Res*., 115, B10101, doi:10.1029/2009JB007184.

Mineral Physics and Chemistry

Burgess, K., R. Cooper, J. Bowles, J. S. Gee, and D. Cherniak (2010), Effects of open and closed system oxidation on texture and magnetic response of remelted basaltic glass, *Geochem. Geophys. Geosys.*, 11, Q10007, doi:10.1029/2010GC003248.

Gialanella, S., F. Girardi, G. Ischia, I. Lonardelli, M. Mattarelli, and M. Montagna (2010), On the goethite to hematite phase transformation, *J. Therm. Anal. Calorim*., 102, 867-873.

Hallstrom, S., L. Hoglund, and J. Agren (2011), Modeling of iron diffusion in the iron oxides magnetite and hematite with variable stoichiometry, *Acta Materialia*, 59, 53-60.

Lu, H. M., and X. Meng (2010), Morin Temperature and Neel Temperature of Hematite Nanocrystals, *J. Phys. Chem. C*, 114, 21291-21295.

Mathieu, R., M. Hudl, and P. Nordblad (2010), Memory and rejuvenation in a spin glass, *Epl*, 90, 67003.

Murad, E. (2010), Mossbauer spectroscopy of clays, soils and their mineral constituents, *Clay Miner.*, 45, 413-430.

Serantes, D., D. Baldomir, M. Pereiro, C. Hoppe, F. Rivadulla, and J. Rivas (2010), Nonmonotonic evolution of the blocking temperature in dispersions of superparamagnetic nanoparticles, *Phys. Rev. B*, 82, 134433.

Vodyanitskii, Y. (2010), Iron Hydroxides in Soils: A Review of Publications, *Eurasian Soil Sci*., 43, 1244-1254.

Vodyanitskii, Y. (2010), Iron minerals in urban soils, *Eurasian Soil Sci.*, 43, 1410-1417.

Instrumentation and Techniques

Kodama, K. (2010), A new system for measuring alternating current magnetic susceptibility of natural materials over a wide range of frequencies, *Geochem. Geophys. Geosys*., 11, Q11002, doi:10.1029/2010GC003303.

Wack, M. (2010), A new software for the measurement of magnetic moments using SQUID and spinner magnetometers, *Comput. Geosci*., 36, 1178-1184.

Zheng, Z., X. X. Zhao, and C. S. Horng (2010), A new high-precision furnace for paleomagnetic and paleointensity studies: Minimizing magnetic noise generated by heater currents inside traditional thermal demagnetizers, *Geochem. Geophys. Geosys*., 11, Q04Y08, doi:10.1029/2010GC003100.

Paleomagnetism and Tectonics

Bilardello, D., and K. Kodama (2010), A new inclination shallowing correction of the Mauch Chunk Formation of Pennsylvania, based on high-field AIR results: Implications for the Carboniferous North American APW path and Pangea reconstructions, *Earth Planet. Sci. Lett*., 299, 218-227.

Caccavari, A., M. Calvo-Rathert, A. Goguitchaichvili, V. Soler, and B. Reyes (2010), A paleomagnetic and rock-magnetic study of a neogene lava flow sequence in La Gomera (Canary Islands, Spain), *Stud. Geophys. Geod.*, 54, 547-560.

Channell, J., D. Hodell, B. Singer, and C. Xuan (2010), Reconciling astrochronological and Ar-40/Ar-39 ages for the Matuyama-Brunhes boundary and late Matuyama Chron, *Geochem. Geophys. Geosys*., 11, Q0AA12, doi:10.1029/2010GC003203.

Kent, D., and E. Irving (2010), Influence of inclination error in sedimentary rocks on the Triassic and Jurassic apparent pole wander path for North America and implications for Cordilleran tectonics, *J. Geophys. Res*, 115, B10103, doi:10.1029/2009JB007205.

Meijers, M., M. Hamers, D. J. J. Van Hinsbergen, D. G. Van Der Meer, A. Kitchka, C. Langereis, and R. Stephenson (2010), New late Paleozoic paleopoles from the Donbas Foldbelt (Ukraine): Implications for the Pangea A vs. B controversy, *Earth Planet. Sci. Lett.*, 297, 18-33.

Morinaga, H., M. Toda, H. Fujino, and N. Hasegawa (2010), Preliminary palaeomagnetic investigation of riverine tufa: is riverine tufa a reliable recorder of the geomagnetic field direction?, *Geophys. J. Int.*, 183, 1231-1238.

Smirnov, A., and J. Tarduno (2010), Co-location of eruption sites of the Siberian Traps and North Atlantic Igneous Province: Implications for the nature of hotspots and mantle plumes, *Earth Planet. Sci. Lett*., 297, 687-690.

Solano, M., A. Goguitchaichvili, L. Bettucci, R. Ruiz, M. Calvo-Rathert, V. C. Ruiz-Martinez, R. Soto, L. M. Alva-Valdivia (2010), Paleomagnetism of early cretaceous arapey formation (Northern Uruguay), *Stud. Geophys. Geod*., 54, 533-546.

Weiss, B., S. Pedersen, I. Garrick-Bethell, S. Stewart, K. Louzada, A. Maloof, N. L. Swanson-Hysell (2010), Paleomagnetism of impact spherules from Lonar crater, India and a test for impact-generated fields, *Earth Planet. Sci. Lett*., 298, 66-76.

Magnetite Verwey Transition, cont'd. from pg. 1

cation substitution), pressure and particle size, and we will describe and explain some surprising and dramatic effects of magnetic fields applied during cooling through T_V.

The Inverse-Spinel Arrangement of Magnetite at $T>T_V$

Like the mineral spinel ($MgAl_2O_4$), many metal oxides including magnetite have a crystallographic structure in which the large O^{2-} ions form a cubic close-packed arrangement and the small metal cations occupy certain "holes" in the oxygen framework. The recurrence interval of the occupancy pattern defines the unit cell, which contains 32 oxygen anions, 8 cations of one metal (the 'X' ions of Verwey and Heilmann [1947]) and 16 'Y' metal ions. Three possible charge-balanced combinations exist: "2-3 spinels" (X^{2+}, Y^{3+}) such as magnetite (Fe^{2+}, Fe^{3+}) and spinel (Mg^{2+}, Al^{3+}), "4-2 spinels" (X^{4+}, Y^{2+}) such as ulvöspinel (Ti^{4+}, Fe^{2+}), and "6-1 spinels" (X^{6+}, Y^{1+}), a combination that Verwey and Heilmann described as "very rare." The cubic spinel structure of magnetite at room temperature was established by the x-ray diffraction work of Bragg in 1915.

The oxygens can be thought of as spheres arranged in sets of hexagonally-packed planes (the (111) planes of the cubic lattice). Each sphere touches six adjoining spheres in the same plane (Fig. 2), as well as three in each of the adjoining layers, making a total of 12 nearest neighbors. Eight tetrahedral voids are formed around each sphere by these nearest neighbors; and since each tetrahedral void is shared by four anions, there are two per O^{2-} in the bulk solid, or 64 per unit cell. Eight of these 64 tetrahedral (or "A") sites contain cations. In a "normal" spinel the A sites are occupied by the X atoms, and in an "inverse" spinel they contain (half of the) Y ions. Octahedral holes ("B" sites) are surrounded by six O^{2-} ions (the vertices of an octahedron); 32 such sites occur in the unit cell and half of them are occupied by cations, which in a normal spinel are the Y ions. In an inverse spinel, the B sites contain the X ions and half of the Y ions, in a generally unordered fashion. Overall the structure can be visualized as a repeating sequence of alternating layers normal to [111] (and symmetrically-equivalent axes): O^{2-} ions, A-site cations, O^{2-} ions, and B-site cations.

Verwey & Heilmann [1947] modeled the stability of normal and inverse spinel structures of different compositions in terms of "Madelung potentials" based on Coulomb attraction and Born repulsion, and predicted that 4-2 spinels should always be inverse (i.e. $Y^{2+}{}_A[X^{4+}Y^{2+}]{}_BO_4$ is a lower-energy, more stable arrangement than $X^{4+}{}_A[2Y^{2+}]{}_BO_4$), having the more strongly-charged cations in the octahedral sites, coordinated with 6 oxygens. They predicted that 2-3 spinels should generally be normal, and found that such was indeed the case for Al^{3+} and Cr^{3+}, but they noted an "abnormal" tendency for Fe^{3+} to form inverse spinels (as it does with Ni^{2+}, Cu^{2+}, Mg^{2+}, Co^{2+}, Mn^{2+} and Fe^{2+}; only Zn^{2+} and Cd^{2+} were found to make normal Fe^{3+} spinels). The competing crystal field energy contributions leads to some cations having site preferences, such as the B-site preference for Ti^{4+}.

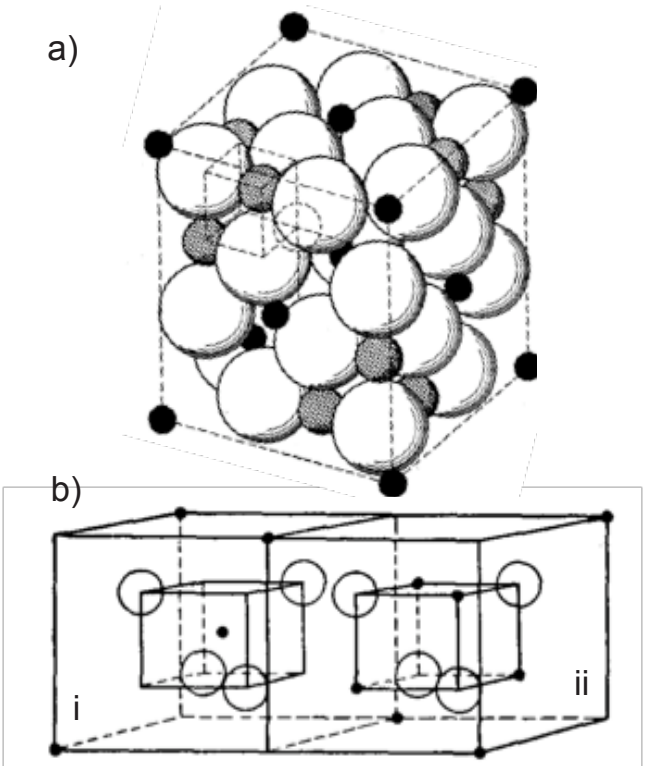

Figure 2. (a) Spinel unit cell, with cubic close-packed O_2 ions (large white spheres) and metal cations in octahedral sites (intermediate-sized hatched spheres), and tetrahedral sites (small black spheres). (b) Spinel sublattices with cations (small black dots) in tetrahedral (i) and octahedral (ii) coordination with neighboring O_2 ions (large circles). The bulk material is "a 3-dimensional packing of A- and B- cubes in a checkerboard arrangement." [Verwey & Heilman, 1947]

The mixed-valence cations in the B sites are responsible for the relatively high electrical conductivity of magnetite, which is classified as a semiconductor. Verwey and his Philips colleagues conducted extensive experiments on conductivity of normal and inverse spinels as a function of composition and of temperature. Verwey & de Boer [1936] found that the room-T conductivity of the inverse spinel magnetite is 10^8-10^9 times greater than those of the normal (but otherwise very similar) spinels Mn_3O_4 and Co_3O_4, and they attributed the difference to the cation valence states and their spatial distributions. Specifically, they proposed that electrons in Fe_3O_4 could move relatively easily from divalent to trivalent ions in the B-site planes, a phenomenon now known as "electron hopping." After receiving an electron in this way, a formerly-ferric (now ferrous) Fe ion can just as easily lose one to another nearby Fe^{3+}, and current can thereby be transported through the lattice. This B-site valence flexibility is often expressed by writing the structural formula as $Fe^{3+}{}_A[2Fe^{2.5+}]{}_BO_4$ [e.g., Piekarz et al., 2007] or as $Fe^{3+}{}_A[2Fe^{3+}+e^-]{}_BO_4$ [e.g., Rozenberg et al., 2006].

This electron hopping is also evident in ^{57}Fe Mössbauer spectroscopy, which is sensitive to the valence, coordination and magnetic ordering of the iron ions in solid materials. In magnetite the three species (tetrahedral Fe^{3+}, octahedral Fe^{2+} and octahedral Fe^{3+}) are effectively reduced to two (tetrahedral Fe^{3+} and octahedral $Fe^{2.5+}$) by electron hopping, and the absorption spectrum therefore shows two distinct sextets. The octahedral-sextet

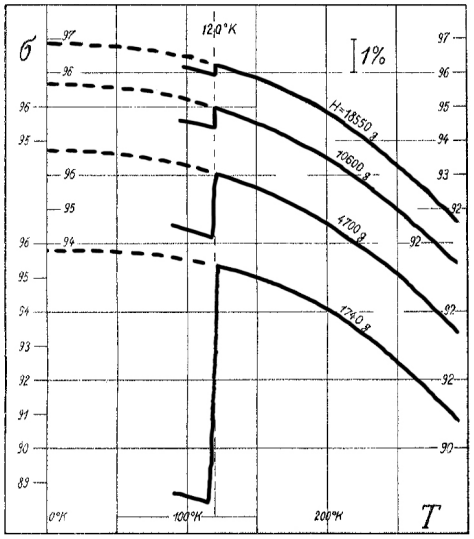

Figure 3. Magnetite magnetization as a function of temperature for various fixed field values. Curves are offset to avoid overlapping. [From Weiss and Forrer, 1929.]

linewidths broaden with increasing T above 300 K, as thermally-activated hopping increases the charge disorder of the B-site cations [Sawatzky et al., 1969].

The inverse-spinel arrangement also accounts for the intensity of spontaneous magnetization in magnetite. Unlike true ferromagnets (e.g. metallic iron), in which neighboring magnetic atoms are directly exchange-coupled, ferrimagnets (like magnetite) are ordered by indirect "superexchange," in which the irons are mutually coupled through intervening oxygens. As first hypothesized by Néel, the result is antiferromagnetic coupling between sublattices. Since the B sites contain twice as many Fe atoms as the A sites, a fairly strong net spontaneous magnetization may be expected. For Fe_3O_4 in the inverse-spinel arrangement, half of the Fe^{3+} ions are in the tetrahedral sublattice and the other half in the antiferromagnetically-coupled octahedral sublattice, so the moments of the trivalent iron atoms are mutually cancelling, and the net spontaneous moment is equal to the uncancelled monents of the Fe^{2+} ions in the B sites. This amounts to ~4 Bohr magnetons ($4\mu_B$) per formula unit (~92 $Am^2\ kg^{-1}$) at room temperature, matching the experimental value determined by Weiss and Forrer in 1929 [see also Duffy et al., 2010]. In contrast, in a normal spinel arrangement, with divalent ions in the tetrahedral sites antiferromagnetically coupled to the trivalent ions (5μB per atom) in the octahedral sites, magnetite's net spontaneous magnetization would be ~$6\mu_B$ per formula unit or 138 $Am^2\ kg^{-1}$ [e.g., Baudelet et al., 2010].

Finally, the inverse spinel structure contributes to magnetite's weak magnetocrystalline anisotropy at $T > T_V$. Magnetocrystalline anisotropy in general arises from a combination of single-ion anisotropy and anisotropic exchange interactions, related to the way that electron orbitals fit into the crystal lattice [e.g., Stacey & Banerjee 1974 1.5; O'Reilly 1984 3.4; Dunlop & Ozdemir 1997 2.8.2]. The details of these mechanisms are beyond the scope of this article, but we note here simply that whereas Fe^{2+} has a strong single-ion anisotropy (related to spin-orbit coupling), Fe^{3+} has none. The inverse spinel cation arrangement (effectively lacking distinct ferrous ions due to B-site electron hopping), together with the cubic crystal symmetry, account for the relatively weak magnetocrystalline anisotropy of magnetite at room temperature. The anisotropy constants K_1 and K_2 describe how magnetic energy varies according to orientation of the magnetization with respect to the cubic lattice. For $K_1<0$ the easy magnetic axes are the body diagonals, as they are for Fe_3O_4 at 300 K. The values of these constants change with composition and temperature [e.g., Kakol et al., 1991]; in Ti-rich titanomagnetites ($Fe_{3-x}Ti_xO_4$; $x > 0.55$) the [100] directions are the easy axes at room T, as is the case for magnetite at temperatures below T_I.

The Verwey Transition: Initial Observations

In his extensive review article, Walz [2002] points to a set of low-temperature magnetic susceptibility measurements by K. Renger in Zurich a century ago (in his thesis work under Weiss and Einstein) as the first observation of the Verwey transition. Weiss & Forrer [1929] measured the magnetization of several magnetite specimens as functions of applied field and temperature and found "une discontinuité singulière" near 120 K (Fig. 3) in all of them, the magnitude of the jump being larger in weaker fields. They wrote that "la nature de cette transformation est inconnue" ("the nature of this transformation is unknown"), but by applying an approach-to-saturation law of the form $M(H)=M_S(1-a/H)$, they established that the values of M_S were essentially identical above and below the transition. However the respective values of *a* showed that magnetite is approximately 10 times harder magnetically just below T_V than it is just above.

In 1939 Verwey published his first account of the sharp increase in the electrical resisivity of magnetite on cooling, at about 120 K (Fig. 4). Aware of the specific heat anomaly previously seen by Parks & Kelly [1926] and the magnetic observations of Weiss & Forrer [1929], Verwey had reason to expect that resistivity might also exhibit interesting changes at low temperature. When he found them he was quick to interpret them in terms of the disordered mixed-valence B-site cation arrangement (which enables current flow at higher temperatures) giving way to a more ordered state at low temperature. He made similar ρ(T) measurements for a cation-deficient magnetite ($FeO:Fe_2O_3 = 1:1.08$), reasoning that the higher ferric/ferrous ratio would affect his postulated mechanisms, and found that the discontinuity disappeared.

Verwey and Haayman [1941] extended these experiments to a series of intermediate stoichiometries, and discovered several regular features that could be interpreted in terms of the mixed-valence cation arrangement in the B sublattice. First, conductivity in the "high-T" state ($T>T_V$) decreases progressively with increasing cation deficiency, from which they deduced: "It is evident that the holes act as negative charge centers which will try to surround themselves by an excess of Fe^{3+}," thus impeding the easy flow of electrons through the lattice. Second, the semiconductor-insulator transition became less sharp, and was shifted to lower temperatures, with increasing

cation deficiency (conductivity changing by a factor of ~100 at ~118 K for stoichiometric magnetite; and by a factor of ~3 at ~100 K for $FeO:Fe_2O_3$ = 1:1.07). To account for the abrupt change in stoichiometric magnetite they tentatively proposed a charge-ordered arrangement of the B-sites in the low-T phase, with Fe occurring in rows of equally-charged (di- and trivalent) ions along [110] directions. Cation deficiency interferes with such charge ordering: "for it is obvious that the presence of irregularly-distributed and frozen-in holes, and their repulsive action upon the surrounding electrons, must counteract and finally inhibit the formation of a regular pattern. A concentration of holes of 1% (corresponding to $FeO:Fe_2O_3$ = 1:1.08) is actually sufficient to suppress the transition entirely."

The Low-T Phase of Magnetite ($T<T_V$)

For their proposed charge-ordered low-T arrangement, Verwey et al. [1947] noted that "without resorting to a larger unit cell, this pattern of order can no longer be of cubic symmetry. The most probable pattern is one having a tetragonal cell…" Early efforts to detect this showed that overall changes in crystal geometry (symmetry and lattice dimensions) are very small across T_V, and difficult to detect by x-ray diffraction. These changes are also difficult to distinguish from charge-ordering effects, and observations are further complicated by twinning. In an important neutron-diffraction study, Hamilton [1958] cooled single-crystal magnetite through T_V in a field applied along the cubic [001] axis to suppress twinning effects, and obtained the following results/conclusions: 1) the low-T phase is orthorhombic; 2) all Fe ions in the orthorhombic phase have their magnetic moments aligned along the cubic [001] direction closest to the direction of the applied cooling field (i.e., this becomes the *c*-axis and unique magnetic easy axis of the low-T phase); 3) the cubic [110] axes (face diagonals) perpendicular to c become the orthorhombic *a* and *b* axes (magnetically hard and intermediate axes, respectively); and 4) the octahedral ferric ions lie in rows parallel to *a* and the ferrous ions in rows parallel to *b* (i.e. exactly the structure proposed by Verwey et al.; see Fig. 5). Samuelson et al. [1968] observed (002) reflections like those found by Hamilton, but also discovered a neutron-polarization sensitivity that led them to a very different interpretation: "…the extra reflections are not due to a purely magnetic ordering (octahedral site ordering or ferrimagnetic spiral structure). Rather they are caused by a lowering of the crystal symmetry…" with a doubling of the unit cell along *c*. Later work demonstrated that the low-temperature phase actually has monoclinic symmetry [e.g. Chikazumi, 1976; Yoshida and Iida, 1976], and while this is now the commonly-assumed structure, the details remain an active topic of research.

The nanoscale configuration of ferrous and ferric ions in low-T magnetite and the processes involved in the transition remain controversial, and current physical models are daunting in their complexity. Although no consensus has emerged on the fundamental mechanisms driving the transformation, it is nevertheless clear that they are far more complicated than the simple charge-ordering model of Verwey et al. In our (oversimplified) understanding, the models fall into two groups. One suggests that the transition is fundamentally a coordination crossover: a reversible transformation between normal $(Fe^{2+}_A[2Fe^{3+}]_BO_4$ for $T<T_V$) and inverse $(Fe^{3+}_A[2Fe^{2.5+}]_BO_4$ for $T>T_V$) spinel arrangements [Rozenberg et al., 2006, 2007] (but see also Baudelet et al [2010]). Other models generally involve some form of incomplete charge ordering of the octahedral iron ions, in combination with ordering of electron-orbital orientations of the ferrous ions, lattice distortion, and other additional complicating factors, and the arguments revolve around the relative importance of the various interacting effects [Walz 2002; Garcia & Subias 2004; Zhou & Ceder 2010; Piekarz et al 2007].

Effects on Magnetic Properties and Measurements

Here we will suspend consideration of the fundamental atomic-scale phenomena and provide a brief overview of the resulting magnetic properties of monoclinic magnetite below T_V. The net spontaneous magnetization changes by only a very small amount (if at all) across the transition, according to bulk magnetization [Weiss & Forrer 1929; Ozdemir & Dunlop 1999], Mössbauer spectroscopy [van der Woude et al., 1968], and x-ray magnetic circular dichroism (XMCD) measurements [Baudelet, 2010]. This appears to be inconsistent with the proposed coordination crossover, and suggests that the structure can still (to a good approximation) be described as an inverse spinel.

The most significant magnetic effect of the transition is a dramatic increase in the magnetocrystalline anisotropy in the low-T phase. The cessation of electron hopping, whatever its ultimate cause, leaves us with distinct ferrous and ferric ions in the B sublattice (in contrast to the $Fe^{2.5+}$ of room-T magnetite), and the Fe^{2+} ions are largely responsible for the strong anisotropy. Low-temperature magnetization curves show that the approach to saturation is much slower along the *a*- and *b*-axis than along *c*; this uniaxial anisotropy is much stronger than the shape anisotropy of even extremely elongate particles [Ozdemir & Dunlop 1999; Carter-Stiglitz et al., 2002].

This abrupt change in anisotropy is fundamentally responsible for magnetite's diagnostic low-T variations

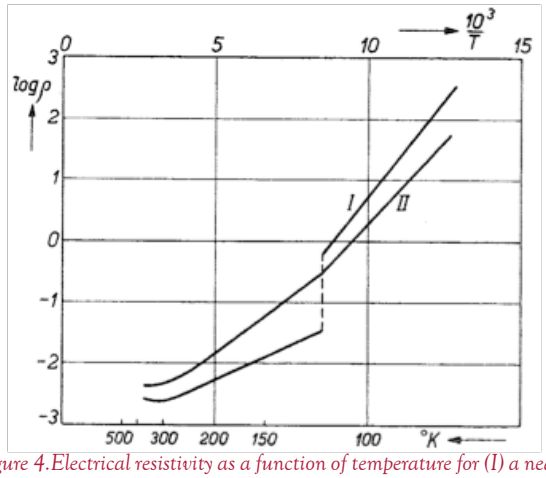

Figure 4.Electrical resistivity as a function of temperature for (I) a nearly stoichiometric magnetite and (II) a cation-deficient magnetite. [From Verwey, 1939]

in susceptibility (k) and remanence. k(T) curves for pure magnetite (Fig. 6a) typically have the form of a step function, with relatively minor variations above and below the transition, and an essentially instantaneous change at T_V[1], with $k_{monoclinic}/k_{cubic} \sim 0.5$. Commonly, the isotropic point is seen as a maximum in k(T). For remanence acquired at low T (Fig. 6b, LTSIRM curve), the behavior on warming is also step-like, with substantial loss of remanence at T_V, typically by 25% to 100%, depending on particle size and shape [e.g. Ozdemir & Dunlop 1999; Carter-Stiglitz et al., 2002]. Strong domain-wall pinning by the high uniaxial anisotropy of the monoclinic phase allows the acquisition and retention of intense remanence below T_V, but domain arrangements are profoundly altered by the loss of this anisotropy on transformation to the cubic phase.

Approaching T_V from above produces quite different remanent magnetization behavior, especially for multidomain magnetites (where magnetocrystalline anisotropy plays a significant role in stabilizing room-T remanence). There is a significant loss of remanence on cooling through T_I (Fig. 6b, RTSIRM curves), but the changes are generally not steplike; there is a continual reorganization of domain geometry in response to the progressively changing anisotropy while cooling [Ozdemir & Dunlop 1999; Dunlop 2003]. In some cases additional changes are seen on continued cooling through T_V, and the behavior is strongly sensitive to factors including grain size, crystal orientation, stoichiometry and the nature of the initial remanence. We will return to these dependencies in subsequent articles.

Mössbauer spectra are distinctly different for $T<T_V$ (Fig. 6c). The octahedral ferrous and ferric ions generate distinct sextets, in contrast to the single $Fe^{2.5+}$ octahedral sextet they form together above T_V. The tetrahedral Fe^{3+} absorption pattern does not change significantly across T_V. The low-T ferric sextets (tetrahedral and octahedral) are strongly overlapping, and can be approximated by a single sextet, which accounts for 2/3 of the total absorption. Sawatzky et al. [1969] found that the best fits at 4.2 K were obtained using four sextets: one each for the A- and B-site Fe^{3+}, and two for the B-site Fe^{2+} (due to the sensitivity of Fe^{2+} to crystal symmetry, related to crystal-field splitting of atomic orbital levels).

Closing Remarks for Part 1

In their 2004 review article, Garcia and Subias stress the fundamental scientific significance of understanding the Verwey transition: "The important fact is that magnetite has been taken as a reference for all the solid state physics developed in the second half of the 20th century." Discontinuous changes in magnetic, electrical and thermal properties coincide with structural changes in the crystal lattice, and possibly with the onset of charge ordering in the octahedral cations and/or electron-orbital ordering of the ferrous ions.

Ultimate causes notwithstanding, the Verwey transition is a phenomenon that provides a surprisingly rich trove of information about natural materials and their origins and history. Stay tuned for future installments in the series, where we will back up this claim.

References

Baudelet, F., S. Pascarelli, O. Mathon, J.-P. Itié, A. Polian, and J.-C. Chervin (2010), Absence of abrupt pressure-induced magnetic transitions in magnetite, *Phys. Rev. B*, 82(140412).

Carter-Stiglitz, B. S., M. J. Jackson, and B. M. Moskowitz (2002), Low-temperature remanence in stable single domain magnetite, *Geophys. Res. Lett.*, 97, 10.1029/2001GL014197.

Chikazumi, S. (1976), Current understanding of low temperature phase transition of magnetite, particularly in relation to the behavior of magnetocrystalline anisotropy, *AIP Conf. Proc.*, 29, 382-387.

Duffy, J. A., J. W. Taylo, S. B. Dugdale, C. Shenton-Taylor, M. W. Butchers, S. R. Giblin, M. J. Cooper, Y. Sakurai, and M. Itou (2010), Spin and orbital moments in Fe_3O_4, *Phys. Rev. B*, 81(134424).

Dunlop, D. J. (2003), Stepwise and continuous low-temperature demagnetization, *Geophys. Res. Lett.*, 30, 10.1029/2003GL017268.

Garcia, J., and G. Subias (2004), The Verwey transition-a new perspective, *J. Phys. Condens. Matter*, 16(7), R145-178.

Hamilton, W. C. (1958), Neutron Diffraction Investigation of the 119°K Transition in Magnetite, Phys. Rev., 110(5), 1050-1057.

Kakol, Z., J. Sabol, and J. M. Honig (1991), Magnetic anisotropy of titanomagnetites $Fe_{3-x}Ti_xO_4$, $0<=x<=0.55$, *Phys. Rev. B*, 44, 2198–2204.

Mauritsch, H. J., and P. Turner (1975), The identification of magnetite in limestones using the low-temperature transition, *Earth Planet. Sci. Lett.*, 24, 414–418.

Merrill, R. T. (1970), Low-temperature treatments of magnetite and magnetite-bearing rocks, *J. Geophys. Res.*, 75, 3343–3349.

Moskowitz, B. M., R. Frankel, and D. Bazylinski (1993), Rock magnetic criteria for the detection of biogenic magnetite, *Earth Planet. Sci. Lett.*, 120, 283–300.

Moskowitz, B. M., R.B. Frankel, D. Bazylinski, H.W. Jannasch, and

[1] Frequently an additional step change is observed near or below 50 K, as in Fig. 6a. This phenomenon will be discussed in a separate future article.

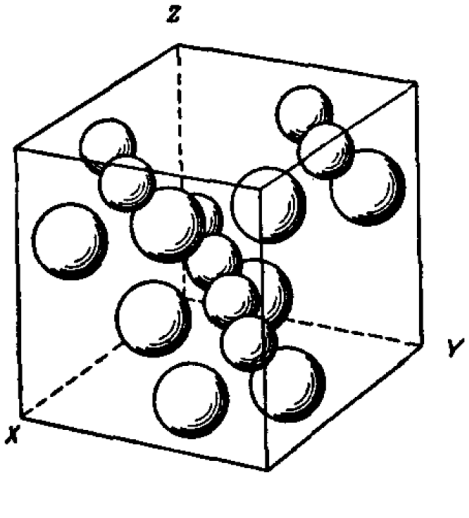

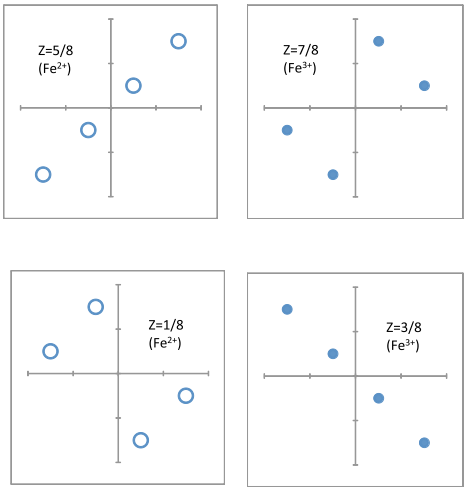

Figure 5. (left) Tetragonal structure proposed by Verwey et al for the low-T phase of magnetite. Only Fe ions in octahedral sites are shown: large spheres are Fe^{2+} and small spheres are Fe^{3+}. Oxygen and tetrahedral iron are omitted for clarity. [From Verwey et al., 1947]. Ferrous and ferric ions occur in alternating (001) planes, aligned along [110] or [-110]. (right) Slices (perpendicular to z) through the structure at left showing the arrangement of cations.

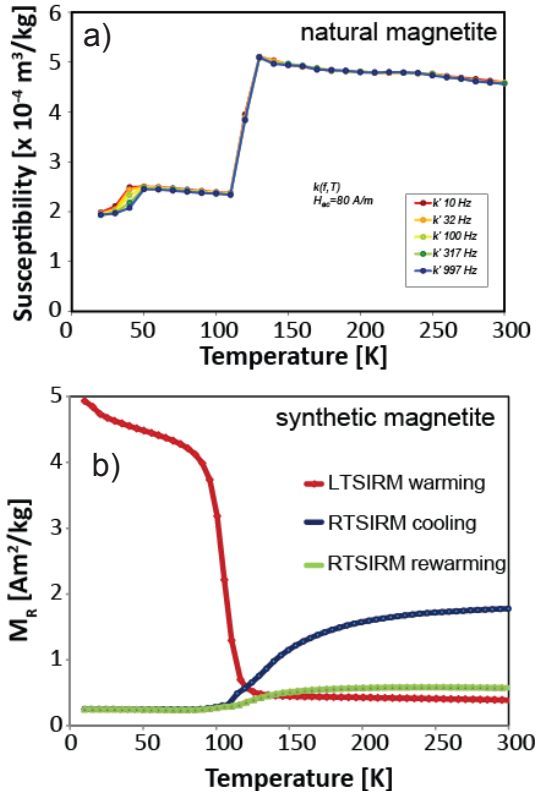

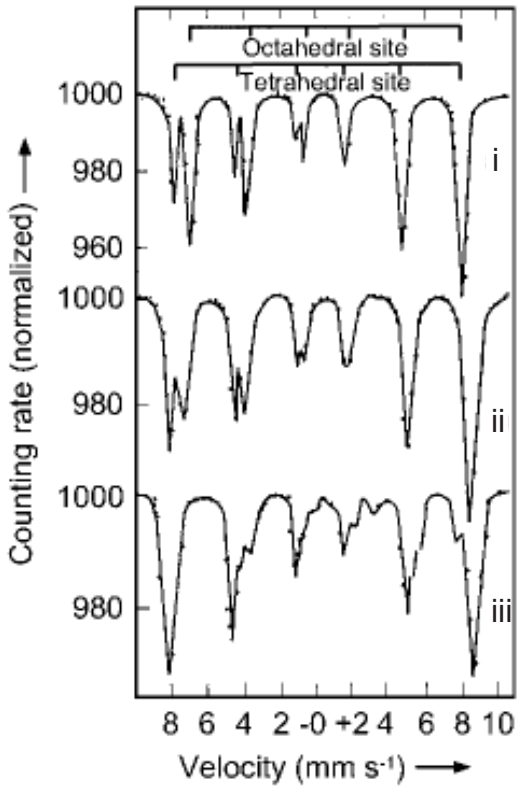

Figure 6. (a) Susceptibility as a function of temperature for a natural magnetite. Varying the frequency of the applied field produces the multiple curves, which overlap at all T > 50 K. (b) Saturation isothermal remanence acquired at 10 K and measured on warming (LTSIRM warming); saturation isothermal remanence acquired at 300 K and measured on cooling to 10 K (RTSIRM cooling) and on warming back to 300 K (RTSIRM rewarming). (c) Mössbauer spectra of Fe_3O_4 at (i) 296 K, (ii) 120 K, and (iii) 83 K [From Walz, 2002].

D.R. Lovley (1989), A comparison of magnetite particles produced anaerobically by magnetotactic and dissimilatory iron-reducing bacteria, *Geophys. Res. Lett.*, 16, 665-668.

Özdemir, Ö., and D. J. Dunlop (1999), Low-temperature properties of a single crystal of magnetite oriented along principal magnetic axes, *Earth Planet. Sci. Lett.*, 165(2), 229-239.

Ozima, M., M. Ozima, and S. Akimoto (1964), Low temperature characteristics of remanent magnetization of magnetite—self-reversal and recovery phenomena of remanent magnetization, *J. Geomagn. Geoelectr.*, 16, 165–177.

Parks, G. S., and K. E. Kelley (1926), The heat capacities of some metallic oxides, *J. Phys. Chem.*, 30, 47-55.

Piekarz, P., K. Parlinski, and A. M. Oles (2007), Origin of the Verwey transition in magnetite: Group theory, electronic structure, and lattice dynamics study, *Phys. Rev. B*, 76(16).

Rozenberg, G. K., Y. Amiel, W. M. Xu, M. P. Pasternak, R. Jeanloz, M. Hanfland, and R. D. Taylor (2007), Structural characterization of temperature- and pressure-induced inverse <-> normal spinel transformation in magnetite, *Phys. Rev. B*, 75.

Rozenberg, G. K., M. P. Pasternak, W. M. Xu, Y. Amiel, M. Hanfland, M. Amboage, R. D. Taylor, and R. Jeanloz (2006), Origin of the Verwey transition in magnetite, *Phys. Rev. Lett.*, 96, 1-4.

Samuelsen, E. J., E. J. Bleeker, L. Dobrzynski, and T. Riste (1968), Neutron Scattering from Magnetite below 119°K, *J. Appl. Phys.*, 39, 1114-1115.

Sawatzky, G. A., J. M. D. Coey, and A. H. Morrish (1969), Mossbauer Study of Electron Hopping in the Octahedral Sites of Fe_3O_4, *J. Appl. Phys.*, 40, 1402-1403.

van der Woude, F., G.A. Sawatzky, and A.H. Morrish, Relation between hyperfine magnetic fields and sublattice magnetization in Fe_3O_4, *Phys. Rev.*, 167, 533-535, 1968.

Verwey, E. J. (1939), Electronic conduction of magnetite (Fe_3O_4) and its transition point at low temperature, *Nature*, 144, 327-328.

Verwey, E. J., and P. W. Haayman (1941), Electronic conductivity and transition point in magnetite, *Physica*, 8, 979-982.

Verwey, E. J., and E. L. Heilmann (1947), Physical properties and cation arrangements of oxides with spinel structure I. Cation arrangement in spinels, *J. Chem. Phys.*, 15, 174-180.

Verwey, E. J., P. W. Haayman, and F. C. Romeijn (1947), Physical properties and cation arrangements of oxides with spinel structure II. Electronic conductivity, *J. Chem. Phys.*, 15, 181–187.

Verwey, E. J. W., and J. H. de Boer (1936), *Rec. Trav. Chim. Pays-Bas*, 55, 531-540.

Walz, F. (2002), The Verwey transition - a topical review, *J. Phys. Condens. Matter*, 14, R285-340.

Weiss, P., and R. Forrer (1929), Absolute Saturation of Ferromagnetic Substances and the Law of Approach as a Function of the Field and of the Temperature, *Ann. Physik*, 12, 279-374.

Yoshida, J., and S. Iida (1977), X-ray diffraction study on the low temperature phase of magnetite, *J. Phys. Soc. Japan*, 42, 230-237.

Zhou, F., and G. Ceder (2010), First-principles determination of charge and orbital interactions in Fe_3O_4, *Phys. Rev. B*, 81(205113).

Evert Johannes Willem Verweij (Verwey)
b. April 30, 1905, Amsterdam
d. February 13, 1981, Utrecht

After completing his doctorate in chemistry at the University of Amsterdam in 1934, Evert Johannes Willem Verweij (aka Verwey) moved to the Philips Research Laboratories (NatLab) in Eindhoven. There, in addition to his work on metal oxides, he continued research into the properties and behavior of colloids for which he is widely remembered today. Verwey lends his name to the so-called DLVO theory, which describes the force balances in stable colloidal suspensions. The details of this theory were developed by Boris Deryagin (1902-1994) and Lev Landau (1908-1969) in Russia and independently by Verwey and Theo Overbeek (1911-2007) in the Netherlands. In 1946 Verwey was appointed director of NatLab (along with Hendrik Casimir and Herre Rinia), a position which he held until 1966. Verwey was elected to the Royal Netherlands Academy of Sciences in 1949.

As a side note, Verwey spent the summer of 1933 working with Izaak Kolthoff at the University of Minnesota, the future home of the Institute for Rock Magnetism!

University of Minnesota
291 Shepherd Laboratories
100 Union Street S. E.
Minneapolis, MN 55455-0128
phone: (612) 624-5274
fax: (612) 625-7502
e-mail: irm@umn.edu
www.irm.umn.edu

Nonprofit Org.
U.S Postage
PAID
Minneapolis, MN
Permit No. 155

The IRM Quarterly

The *Institute for Rock Magnetism* is dedicated to providing state-of-the-art facilities and technical expertise free of charge to any interested researcher who applies and is accepted as a Visiting Fellow. Short proposals are accepted semi-annually in spring and fall for work to be done in a 10-day period during the following half year. Shorter, less formal visits are arranged on an individual basis through the Facilities Manager.

The *IRM* staff consists of **Subir Banerjee**, Professor/Founding Director; **Bruce Moskowitz**, Professor/Director; **Joshua Feinberg**, Assistant Professor/Associate Director; **Jim Marvin**, Emeritus Scientist; **Mike Jackson**, **Peat Sølheid**, and **Julie Bowles**, Staff Scientists.

Funding for the *IRM* is provided by the **National Science Foundation**, the **W. M. Keck Foundation**, and the **University of Minnesota**.

The *IRM Quarterly* is published four times a year by the staff of the *IRM*. If you or someone you know would like to be on our mailing list, if you have something you would like to contribute (*e.g.*, titles plus abstracts of papers in press), or if you have any suggestions to improve the newsletter, please notify the editor:

Julie Bowles
Institute for Rock Magnetism
University of Minnesota
291 Shepherd Laboratories
100 Union Street S. E.
Minneapolis, MN 55455-0128
phone: (612) 624-5274
fax: (612) 625-7502
e-mail: jbowles@umn.edu
www.irm.umn.edu